

Measurements of the proton total reaction cross section for light nuclei between 20 and 48 MeV*

W. F. McGill[†]

Department of Physics, University of California, Los Angeles, California 90024

R. F. Carlson[‡]

*Department of Physics, University of Redlands, Redlands, California 92373 and
Department of Physics, University of California, Los Angeles, California 90024*

T. H. Short^{‡§}

Department of Physics, University of Redlands, Redlands, California 92373

J. M. Cameron,[¶] J. Reginald Richardson, I. Šlaus,^{||}

W. T. H. van Oers,^{**} and J. W. Verba^{††}

Department of Physics, University of California, Los Angeles, California 90024

D. J. Margaziotis^{***}

Department of Physics, California State University, Los Angeles, California 90032

P. Doherty

Department of Physics, Loyola University, Los Angeles, California 90045

(Received 19 September 1974)

Measurements of proton total reaction cross sections for ${}^9\text{Be}$, C, ${}^{19}\text{F}$, ${}^{27}\text{Al}$, and Si have been made in the energy range 20 to 48 MeV. These measurements were made using a variation of a standard attenuation technique. The cross sections are compared with various theoretical predictions.

[NUCLEAR REACTIONS ${}^9\text{Be}$, C, ${}^{19}\text{F}$, ${}^{27}\text{Al}$, Si; 20 MeV < T < 48 MeV, between 8
and 14 measurements for each nucleus, measured: σ_R ; natural targets.]

I. INTRODUCTION; MOTIVATION

When a nucleon interacts with a nucleus, only two possibilities exist: The nucleon will either be elastically scattered or it will initiate a reaction (including inelastic scattering). Hence, one of the fundamentally important experiments in nuclear physics is the measurement of total reaction cross sections.

Specifically, total reaction cross sections are of importance in the following areas.

(i) Optical model studies. The large amount of existing data on the elastic scattering of nucleons from medium and heavy nuclei has been successfully described by the optical model.¹ This model replaces the aggregate of nucleons with a potential having several components: a complex central potential plus a complex spin-orbit potential. The optical potential can be interpreted in terms of macroscopic features of the nucleus such as the matter and charge distributions.² The optical model assumes a uniform potential representing the nucleon-nucleus interactions, and it further assumes that the nuclear energy levels of

the compound system are close together so that isolated resonances are not experimentally observed. These assumptions are not clearly justified for very light nuclei interacting with nucleons of energies up to 40 MeV. Studies in this energy region can thus help to determine the limits of validity of the model and might indicate the need for modifications. As an example, the study of elastic scattering of protons from carbon below 30 MeV^{3,4} has required the use of Breit-Wigner resonance terms in addition to the optical model potential.^{5,6}

Optical model studies^{1,7-10} have indicated that its parameters vary with energy in a systematic way. To study the form of this variation, a set of measurements of the elastic differential cross sections, the polarizations, and the total reaction cross section is needed over a wide range of energies. In particular, the imaginary parameters of the optical potential are quite sensitive to the total reaction cross section.

(ii) Few nucleon studies. Next to the elastic scattering angular distributions, the most important experimental parameter to be reproduced by theory is the total reaction cross section.

Recently nucleon-deuteron disintegration cross sections have been calculated within the Faddeev formalism.^{11,12} Total reaction cross section measurements for very light nuclei should prove useful in distinguishing between such calculations. In addition total reaction cross sections provide an important constraint on phase shift analyses of nucleon elastic scattering.

To carry out measurements of proton total reaction cross sections, a method has been developed which is a variant of a standard attenuation technique. The details of this method are reported elsewhere.¹³

In a previous paper,¹⁴ we have reported proton-deuteron total reaction cross sections in the energy range 20–50 MeV. In the present experiment, we have been concerned with optical model studies for light nuclei. Our study of the validity of the optical model for light nuclei began with the measurement of elastic scattering differential cross sections for 46 MeV protons on ⁹Be and

C.^{15,16} The results reported here complete and expand upon those studies. In particular, measurements were made of the proton total reaction cross sections for ⁹Be, C, ¹⁹F, ²⁷Al, and Si between 20 and 48 MeV at the University of California Los Angeles 50 MeV Cyclotron Laboratory.

Proton total reaction cross section data for light elements were not plentiful in this energy region. No measurements existed for fluorine, while silicon was represented by a single measurement. Most of the existing measurements for beryllium, carbon, and aluminum were at energies below 25 MeV. The available data, along with our results, are summarized in Fig. 1.

II. EXPERIMENTAL METHOD

The experiment was performed using a variation of a standard attenuation technique. A tightly collimated and momentum analyzed proton beam [with an energy spread of 150 keV full width at half-maximum (FWHM)] was transported to the total reaction cross section apparatus, a schematic diagram of which is shown in Fig. 2. Plastic scintillator passing detectors 1 and 2 along with annular detectors 3 and 4 provide the trigger signal, $(1\ 2\ \bar{3}\ \bar{4})$, denoted I_0 , for an incident proton unscattered by the passing detectors. After passing through the target, the protons or reaction products may enter the stopping detector telescope, composed of the small plastic disk detector 5 and the CsI(Na) stopping detector 6. All charged particles entering detector 5 are accepted, while discrimination of the signal from detector 6 selects elastically scattered protons plus (depending on the particular nucleus) a few inelastic groups and a small fraction of the continuum. The presence of an OR signal $(5+6)$ represents a nonattenuation event I which in most cases is an unscattered proton, but which can also be an elastically scattered proton with $\theta \leq 45^\circ$ (the maximum acceptance angle of detector 6), or an inelastic event with $\theta \leq 9^\circ$ (the maximum acceptance angle of detector 5). The difference $(I_0 - I)$ is measured directly and corresponds to attenuation events. This difference can be related to the total reaction cross section

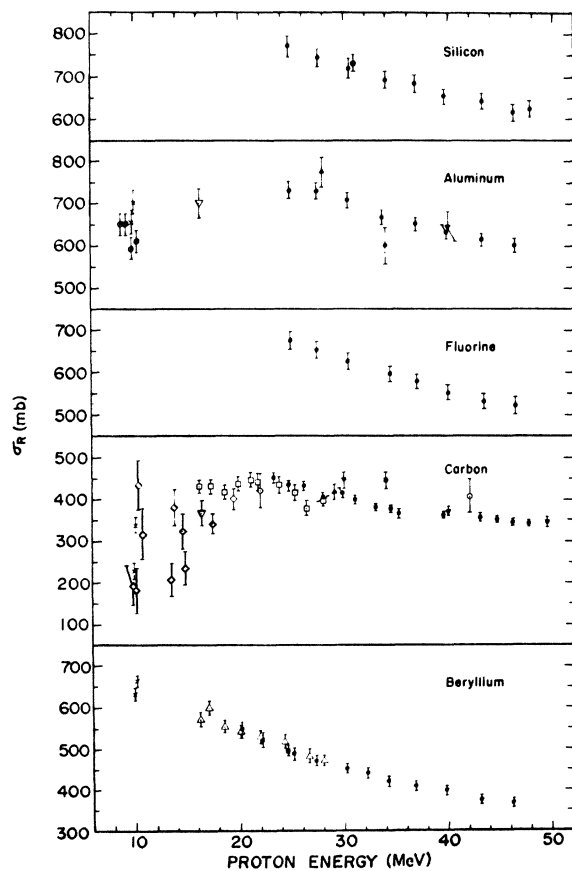


FIG. 1. Proton total reaction cross sections for light nuclei. Legend: \times , Ref. 17; \triangle , Ref. 18; ∇ , Ref. 19; \square , Ref. 20; \diamond , Ref. 21; \circ , Ref. 22; \blacktriangle , Ref. 23; \blacktriangledown , Ref. 24; \blacksquare , Ref. 25; \blacklozenge , Ref. 26; \otimes , Ref. 27; \oplus , Ref. 28; and \bullet , present work.

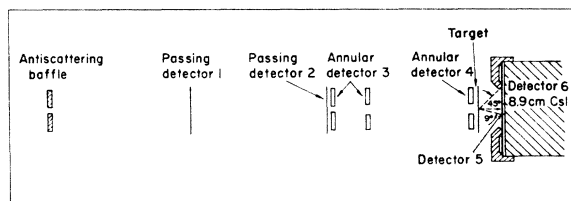


FIG. 2. Schematic diagram of the total reaction cross section apparatus.

after a number of corrections have been applied. The most important corrections are for:

- (i) Elastic scattering events: Protons scattered with angles greater than 45° do not enter detectors 5 or 6 and are counted as attenuation events.
- (ii) Charged particle reaction products (a): Charged particle reaction products entering the stopping detector 6 with energies above the energy corresponding to the threshold of this detector are counted experimentally as nonattenuation events.
- (iii) Charged particle reaction products (b): All charged particle reaction products entering detector 5 are counted as nonattenuation events.
- (iv) Nuclear reactions in the detector 6 scintillator: Protons which elastically scatter into detector 6 and which initiate a nuclear reaction in the scintillator may be counted as attenuation events.

The experiment consisted of a series of target "in" and target "out" measurements at each energy. The energy was varied in steps of about 3 MeV between 20 and 48 MeV. The energy of the incident beam was obtained from a calibration of the bending magnet located upstream from the total reaction cross section apparatus. The calibration was obtained from a series of energy measurements. The energies were determined by comparing the energy of the proton beam degraded through silicon absorbers with the known α -particle lines in the spectra of ^{241}Am , ^{212}Bi , and ^{212}Po sources. Using this method the uncertainty of the incident proton beam was estimated to be ± 150 keV. Please see Ref. 13 for details of the experimental method.

III. TARGETS

In the present experiment only solid targets were used. The beryllium and aluminum targets were fabricated from stock specified to be 99.99% pure or better. The carbon target was made from reactor grade graphite, and the silicon target was formed from material containing less than 100 parts per million of impurities. The C_2F_4 target was cut from commercial teflon stock about which no purity information could be obtained.

Reaction cross section measurements are fairly insensitive to small concentrations of impurities. In the present experiment, contributions due to impurities were neglected.

The thickness of the targets was determined by two methods. First, the targets were measured by a micrometer. Second, the targets were weighed, and since each target was circular in shape, the diameters of the disk were measured. The areal density was then calculated. The weight determination was performed on an electronic balance and was accurate to ± 0.001 g. The measurement of

the diameter was accurate to ± 0.001 cm. The error in the areal density measurements by the second method was a few tenths of a percent. All such measurements agreed with the measurements of the first method to within 1%. The proton energy loss in the targets was on the order of 1 MeV.

In order that the areal density determination be of any significance, the uniformity of the targets must be determined. The silicon target was lapped, polished, and then tested optically; the nonuniformity of this target was less than 0.1%. The uniformity of the beryllium, carbon, and aluminum foils was investigated with an electronic height gauge which is capable of detecting variations of ± 0.00003 cm. Each of the three foils varied by less than 0.0001 cm over its entire surface. The C_2F_4 target was found to be uniform to within 1%. The uncertainty in the value of the areal densities was taken to be 1%. Table I summarizes the measurements of the areal density.

IV. RESULTS

A. Data reduction

The total number of reaction events for both target in and target out were found. The uncorrected cross sections were then calculated using the formula

$$\sigma_{un} = \frac{(I_0 - I)}{nx I_0} - \frac{(i_0 - i)}{nxi_0} ,$$

where $(I_0 - I)$ is the number of attenuation events for I_0 incident protons with the target in; $(i_0 - i)$ is the same as $(I_0 - I)$ but for the target out; and nx is the number of nuclei per cm^2 in the target. The corrections for elastic scattering events, charged particle reactions products, and reactions in the $\text{CsI}(\text{Na})$ scintillator were then applied to σ_{un} to produce the final value of the reaction cross section σ_R .

The reaction cross section for fluorine was computed using the expression

$$\sigma_R = \frac{1}{4} (\sigma_{\text{C}_2\text{F}_4} - 2\sigma_C) ,$$

where $\sigma_{\text{C}_2\text{F}_4}$ and σ_C are the corrected values of

TABLE I. Areal densities of targets.

Target	ρx (mg/cm ²)	nx (nuclei/cm ² $\times 10^{21}$)
Be	80.99	5.412
C	78.87	3.955
C_2F_4	55.83	0.3362
Al	67.27	1.502
Si	78.03	1.673

TABLE II. Example of the comparison of the elastic scattering correction for proton beams of various dimensions.

Beam spot radius (cm)	Elastic correction (central axis calc.) (mb)
0.000	22.4220
0.003	22.4220
0.005	22.4220
0.008	22.4221
0.025	22.4226
0.130	22.4335
0.250	22.4716
0.510	22.6863
1.270	26.8403
2.030	41.8268

the reaction cross section of teflon and carbon, respectively.

B. Corrections

1. Principal corrections

The elastic corrections were obtained by integrating angular distributions of elastic scattering differential cross sections from 45° to 180° . The data for these and the charged particle reaction product correction (a) were obtained from various sources^{3, 15, 16, 29-44}; when adequate data did not exist, the appropriate measurements were made.^{45, 46} The relative error in the elastic correction was taken to be $\pm 7\%$.

The charged particle reaction product correc-

tion (a) was obtained by integrating angular distributions of relevant charged particle data above the detector 6 threshold setting (approximately 6 MeV below the elastic energy) and over the angular range 9° to 45° . The data used are included in the references cited above in the discussion of the elastic corrections.

The charged particle reaction product correction (b) was calculated. Data relevant to the stopping detector 6 reaction correction were both measured and calculated.

Details of the methods of determining the corrections mentioned above are found in Ref. 13.

2. Other corrections

a. Finite target thickness correction. The elastic and charged particle reaction product corrections applied to the uncorrected cross sections correspond to the energy of the incident proton at the center of the target. The proton energy changes by about 1 MeV as it traverses the target, and thus it must be determined whether the actual value of the correction to be applied is equal to the value calculated for the energy of the incident proton at the center of the target. The corrections appear to be smooth functions of energy; averaging the corrections at $(T + 0.5 \text{ MeV})$ and $(T - 0.5 \text{ MeV})$ gives a correction which differs by less than 1 mb from the correction at T . Thus, this effect was regarded as insignificant.

b. Finite beam size correction. The calculation performed to obtain the elastic correction assumes that the proton beam has an infinitesimal cross section, with all protons passing through the center

TABLE III. Proton total reaction cross sections for beryllium.

Energy (MeV)	σ (uncorrected) (mb)	Elastic correction (mb)	Charged particle reaction products correction (a) ^a (mb)	Charged particle reaction products correction (b) ^b (mb)	Correction for reactions in the stopping detector (mb)	σ_R (mb)
46.2	353 ± 5	-11 ± 1	+22 ± 6	+9 ± 9	-6 ± 2	367 ± 12
43.1	356 ± 5	-11 ± 1	27 ± 7	8 ± 8	-5 ± 1	375 ± 12
39.7	382 ± 5	-13 ± 1	24 ± 6	9 ± 9	-4 ± 1	398 ± 12
36.8	398 ± 5	-18 ± 1	26 ± 6	9 ± 9	-4 ± 1	410 ± 12
34.2	410 ± 5	-24 ± 2	31 ± 8	8 ± 8	-4 ± 1	421 ± 13
32.2	430 ± 5	-29 ± 2	39 ± 10	6 ± 6	-4 ± 1	442 ± 13
30.2	452 ± 5	-36 ± 3	34 ± 8	8 ± 8	-4 ± 1	454 ± 13
27.3	481 ± 6	-47 ± 3	35 ± 9	8 ± 8	-3 ± 1	474 ± 14
25.1	493 ± 7	-57 ± 4	50 ± 12	6 ± 6	-3 ± 1	489 ± 16
24.5	510 ± 6	-59 ± 4	41 ± 10	7 ± 7	-2 ± 1	497 ± 14
22.1	535 ± 7	-72 ± 5	56 ± 14	6 ± 6	-2 ± 1	523 ± 18
20.1	565 ± 8	-83 ± 6	60 ± 15	6 ± 6	-1 ± 1	547 ± 19

^a The variation from energy to energy for this correction is due in part to variations in threshold settings for detector 6 for some of the experimental runs.

^b The variation from energy to energy for this correction is due in part to different detector 5 geometries for some of the experimental runs.

TABLE IV. Proton total reaction cross sections for carbon.

Energy (MeV)	σ (uncorrected) (mb)	Elastic correction (mb)	Charged particle reaction products correction (a) ^a (mb)	Charged particle reaction products correction (b) ^b (mb)	Correction for reactions in the stopping detector (mb)	σ_R (mb)
47.7	345 ± 4	-19 ± 1	+14 ± 3	+10 ± 5	-9 ± 2	341 ± 7
46.1	362 ± 6	-21 ± 2	4 ± 1	9 ± 4	-10 ± 2	344 ± 8
44.6	357 ± 4	-24 ± 2	16 ± 4	10 ± 5	-8 ± 2	351 ± 8
43.0	364 ± 5	-27 ± 2	22 ± 6	6 ± 3	-9 ± 2	356 ± 9
39.5	384 ± 5	-38 ± 3	15 ± 4	8 ± 4	-8 ± 2	361 ± 8
35.2	391 ± 7	-57 ± 4	32 ± 8	6 ± 3	-7 ± 1	365 ± 12
34.4	418 ± 5	-61 ± 4	18 ± 4	9 ± 5	-6 ± 1	378 ± 9
33.0	430 ± 6	-64 ± 5	14 ± 3	7 ± 4	-6 ± 1	381 ± 9
31.0	437 ± 6	-67 ± 5	28 ± 7	7 ± 4	-6 ± 1	399 ± 11
29.8	456 ± 6	-72 ± 5	26 ± 6	8 ± 4	-5 ± 1	413 ± 11
27.9	484 ± 6	-95 ± 7	11 ± 3	9 ± 4	-4 ± 1	405 ± 11
26.1	514 ± 7	-98 ± 7	11 ± 3	9 ± 4	-4 ± 1	432 ± 11
24.7	504 ± 7	-102 ± 7	25 ± 6	8 ± 4	-3 ± 1	432 ± 12
23.2	540 ± 6	-121 ± 8	29 ± 7	7 ± 4	-3 ± 1	452 ± 13

^a The variation from energy to energy for this correction is due in part to variations in threshold settings for detector 6 for some of the experimental runs.

^b The variation from energy to energy for this correction is due in part to different detector 5 geometries for some of the experimental runs.

of the target. The finite size of the proton beam introduces a second order correction. For example, a proton passing through the target off center may be scattered elastically at an angle greater than 45° and still enter detector 6; it is also possible that a proton be scattered at an angle less than 45° and not enter detector 6.

The effects of the finite beam size on the elastic correction were studied by computer simulation. The results of this calculation for proton beams of different diameter are indicated in Table II. Since the beam spot size was approximately 0.13 by 0.19 cm, the effect is apparently negligible.

C. Uncertainties in the final result

The principal sources of error in the experiment are the statistical uncertainty in $(I_0 - I)$ and $(i_0 - i)$, the statistical error in subtracting $(i_0 - i)$ from $(I_0 - I)$ to determine the uncorrected cross section, the uncertainty in the correction terms, and the uncertainty in the measurement of the target thickness. The statistical uncertainty can be reduced to 1% by choosing a suitable counting time. The error due to the uncertainty in the target areal density was combined quadratically with the statistical uncertainty in the quantities

TABLE V. Proton total reaction cross sections for fluorine.

Energy (MeV)	σ (uncorrected) (mb)	Elastic correction (mb)	Charged particle reaction products correction (a) ^a (mb)	Charged particle reaction products correction (b) ^b (mb)	Correction for reactions in the stopping detector (mb)	$\sigma_R(C_2F_4)$ (mb)	$\sigma_R(C)$ (mb)	$\sigma_R(F)$ (mb)
46.3	2900 ± 47	-148 ± 11	+55 ± 17	+57 ± 40	-91 ± 46	2773 ± 80	343 ± 7	522 ± 20
43.3	2969 ± 44	-186 ± 13	83 ± 25	45 ± 31	-73 ± 37	2838 ± 71	355 ± 8	532 ± 18
39.9	3124 ± 45	-223 ± 16	46 ± 14	54 ± 38	-73 ± 37	2928 ± 73	361 ± 8	552 ± 18
36.9	3258 ± 47	-264 ± 19	47 ± 14	52 ± 37	-50 ± 25	3044 ± 69	363 ± 11	579 ± 18
34.3	3401 ± 48	-319 ± 23	47 ± 14	51 ± 36	-41 ± 21	3139 ± 69	378 ± 9	596 ± 18
30.4	3630 ± 48	-441 ± 32	115 ± 34	41 ± 29	-31 ± 17	3318 ± 75	405 ± 11	626 ± 19
27.4	3851 ± 53	-536 ± 38	106 ± 32	39 ± 27	-23 ± 12	3438 ± 78	410 ± 10	654 ± 20
24.9	4023 ± 57	-619 ± 43	138 ± 41	35 ± 24	-15 ± 8	3562 ± 86	429 ± 12	676 ± 22

^a The variation from energy to energy for this correction is due in part to variations in threshold settings for detector 6 for some of the experimental runs.

^b The variation from energy to energy for this correction is due in part to different detector 5 geometries for some of the experimental runs.

TABLE VI. Proton total reaction cross sections for aluminum.

Energy (MeV)	σ (uncorrected) (mb)	Elastic correction (mb)	Charged particle reaction products correction (a) ^a (mb)	Charged particle reaction products correction (b) ^b (mb)	Correction for reactions in the stopping detector (mb)	σ_R (mb)
46.3	639 ± 10	-37 ± 3	+13 ± 4	+20 ± 10	-35 ± 7	600 ± 17
43.2	658 ± 9	-48 ± 3	13 ± 4	21 ± 11	-29 ± 6	615 ± 16
39.8	679 ± 10	-61 ± 4	19 ± 6	19 ± 10	-23 ± 4	633 ± 16
36.9	705 ± 10	-72 ± 5	13 ± 4	22 ± 11	-17 ± 3	651 ± 16
33.7	732 ± 11	-87 ± 6	13 ± 4	23 ± 11	-13 ± 3	668 ± 17
30.4	785 ± 11	-107 ± 8	22 ± 7	19 ± 10	-10 ± 2	709 ± 18
27.4	829 ± 12	-130 ± 9	21 ± 6	19 ± 10	-8 ± 2	731 ± 19
24.8	850 ± 12	-156 ± 11	27 ± 8	18 ± 9	-6 ± 1	733 ± 20

^a The variation from energy to energy for this correction is due in part to variations in threshold settings for detector 6 for some of the experimental runs.

^b The variation from energy to energy for this correction is due in part to different detector 5 geometries for some of the experimental runs.

($I_0 - I$) and ($i_0 - i$). This yielded the uncertainty in the uncorrected reaction cross section. This uncertainty was then folded quadratically with the uncertainties in the various corrections, giving the total uncertainty in the final value of σ_R .

The value of σ_R for the chemical compound C_2F_4 and its uncertainty were calculated as for the other nuclei. The uncertainty in the value of σ_R for fluorine was obtained by quadratically combining the errors for C_2F_4 and twice carbon and then dividing by 4.

The results of the measurements and the associated uncertainties (of the order 2–3%) are listed in Tables III through VII; the results, along with measurements from other laboratories, are plotted in Figs. 1 and 3.

V. DISCUSSION

A. Introduction

Recent optical studies have attempted to keep the geometrical parameters fixed and have concentrated on the energy dependence of the potentials. Earlier studies attempted to find best fits by varying all or most of the parameters. In addition, some studies have used a derivative form of the surface absorption, while others used a Gaussian form. Thus, it is rather difficult to compare the various studies. In this section we compare the measured reaction cross sections for 9Be , C, ^{19}F , ^{27}Al , and Si with the theoretical results without a detailed description of the parameter sets used. Values of σ_R at energies other than those measured in the experiment were obtained by

TABLE VII. Proton total reaction cross sections for silicon.

Energy (MeV)	σ (uncorrected) (mb)	Elastic correction (mb)	Charged particle reaction products correction (a) ^a (mb)	Charged particle reaction products correction (b) ^b (mb)	Correction for reactions in the stopping detector (mb)	σ_R (mb)
47.8	627 ± 8	-30 ± 2	+24 ± 5	+22 ± 17	-17 ± 3	626 ± 19
46.2	624 ± 11	-34 ± 2	24 ± 5	20 ± 15	-19 ± 4	615 ± 20
43.2	653 ± 9	-40 ± 3	25 ± 5	21 ± 16	-16 ± 3	643 ± 19
39.6	676 ± 9	-54 ± 4	27 ± 5	19 ± 15	-15 ± 3	653 ± 19
36.8	714 ± 10	-67 ± 5	30 ± 6	19 ± 15	-11 ± 2	685 ± 20
34.0	733 ± 10	-83 ± 6	33 ± 7	20 ± 15	-9 ± 2	694 ± 20
30.5	778 ± 11	-107 ± 8	37 ± 8	19 ± 15	-7 ± 1	720 ± 22
27.5	819 ± 11	-129 ± 9	41 ± 8	19 ± 15	-5 ± 1	745 ± 22
24.7	862 ± 12	-150 ± 11	44 ± 9	19 ± 15	-4 ± 1	771 ± 24

^a The variation from energy to energy for this correction is due in part to variations in threshold settings for detector 6 for some of the experimental runs.

^b The variation from energy to energy for this correction is due in part to different detector 5 geometries for some of the experimental runs.

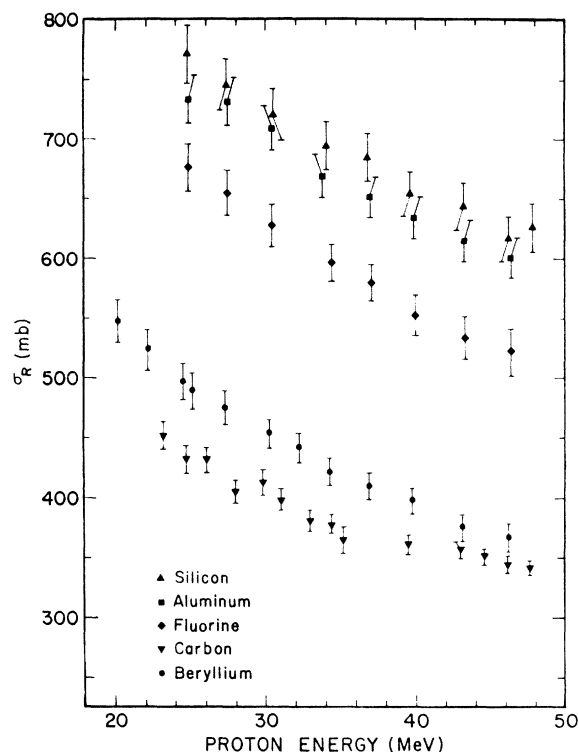


FIG. 3. Results of the present experiment: Proton total reaction cross sections plotted as a function of proton energy.

interpolation; these interpolated values are enclosed in parentheses.

B. Beryllium

Three optical model studies exist of ^9Be , the lightest nucleus investigated in the present experiment. Melkanoff *et al.*⁴⁷ analyzed elastic differen-

TABLE VIII. Comparison of theoretical and experimental values of σ_R for beryllium.

Energy (MeV)	σ_R (theory) (mb)	Reference	σ_R (present experiment) ^a (mb)
46	501	48	367 ± 12
46	449	48	367 ± 12
31.5	318	47	(446)
31.3	495	30	(447)
31.3	464	30	(447)
29.1	483	30	(462)
29.1	495	30	(462)
25	516	30	489 ± 16
25	495	30	489 ± 16
21	526	30	(537)
21	535	30	(537)

^a The results in parentheses have been obtained by interpolation.

tial cross section data at 31.5 MeV. A study of differential cross section and polarization data at 46 MeV was made by Satchler⁴⁸ using various combinations of the available data. Montague *et al.*³⁰ have analyzed elastic differential cross sections and some polarization data between 17 and 31 MeV, using three different parameter sets. We include comparisons with the two sets corresponding to best χ^2 for the elastic fits. Table VIII is a comparison of the various theoretical results and our measured values.

C. Carbon

A fairly large number of optical model analyses exist for ^{12}C for incident energies between 30 and 46 MeV. Table IX provides a comparison with the measured values, and the agreement is fair over the entire region. The studies of Fannon *et al.*,³⁸ Barrett *et al.*,⁴⁹ and Glassgold and Kellogg⁵⁰ provide more than one prediction of σ_R by using various combinations of surface and volume absorption. A complete study of the carbon data using coupled channel calculations should provide a clearer picture of the scattering from this nucleus.

D. Fluorine

Only one study of fluorine was previously made. A limited amount of elastic scattering differential cross section data at 31.5 MeV was analyzed,⁴⁷ and the resulting predicted value of σ_R was 540 mb. This is in poor agreement with our values of 626 ± 19 mb measured at 30.4 MeV and 596 ± 18 mb

TABLE IX. Comparison of theoretical and experimental values of σ_R for carbon.

Energy (MeV)	σ_R (theory) (mb)	Reference	σ_R (present experiment) ^a (mb)
46	350	48	344 ± 8
40	372	37	(360)
40	316	9	(360)
40	324	38	(360)
40	251	38	(360)
40	381	50	(360)
40	314	50	(360)
40	382	51	(360)
31.5	390	47	(395)
31.1	401	36	399 ± 11
30.3	364	49	(407)
30.3	386	49	(407)
30.3	440	49	(407)
30	425	38	413 ± 11
30	424	51	413 ± 11

^a The results in parentheses have been obtained by interpolation.

TABLE X. Comparison of theoretical and experimental values of σ_R for aluminum.

Energy (MeV)	σ_R (theory) (mb)	Reference	σ_R (present experiment) (mb) ^a
46	584	46	600 ± 17
40	638	52	633 ± 16
40	648	52	633 ± 16
40	680	50	633 ± 16
40	705	50	633 ± 16
40	707	46	633 ± 16
34.1	766	46	(666)
31.5	685	47	(695)
30	721	46	709 ± 18
28	719	46	(727)
24.5	724	46	733 ± 20

^a The results in parentheses have been obtained by interpolation.

measured at 34.3 MeV. Further measurements should be made of the elastic differential cross sections and polarization distributions at several energies.

E. Aluminum

Theoretical and experimental values of σ_R for ²⁷Al are compared in Table X. Agreement in general is good for this nucleus, and in some cases it is excellent. A number of analyses exist at 40 MeV,^{46, 50, 52} and the different predicted values reflect the various forms of the potentials which were used.

The elastic differential cross sections measured for use in the elastic corrections were analyzed along with other data at 17.0 and 61.2 MeV. Both surface and volume absorption terms were required in the imaginary part of the optical potential. A set of average geometrical parameters was first determined, and the geometrical parameters were held fixed in the subsequent analysis in order to investigate the energy dependent behavior of the dynamical parameters. The strength of the real central potential was found to decrease with increasing energy of the incident proton, with the energy dependence being represented by $dV/dT \approx -0.30$. The predicted σ_R results are included in the table. Details of this optical model analysis are given in Ref. 46.

F. Silicon

Table XI provides a comparison of the theoretical and experimental values of σ_R for silicon. Agreement is reasonably good for all of the data.

The elastic differential cross sections measured for use in the elastic corrections were analyzed

TABLE XI. Comparison of theoretical and experimental values of σ_R for silicon.

Energy (MeV)	σ_R (theory) (mb)	Reference	σ_R (present experiment) (mb) ^a
46	618	46	615 ± 20
40	630	9	653 ± 19
40	687	46	653 ± 19
34.1	686	46	694 ± 20
31.5	703	47	(713)
30.3	700	44	720 ± 22
30.3	704	44	720 ± 22
30	717	9	720 ± 22
30	710	46	720 ± 22
28	783	46	745 ± 22
24.5	757	46	771 ± 24

^a The results in parentheses have been obtained by interpolation.

along with other data at 28.0 and 30.3 MeV.⁴⁶ The predicted σ_R results are included in the table.

VI. CONCLUSION

The reaction cross sections (Figs. 1 and 3) for the nuclei under study appear to be smoothly decreasing functions of energy in this energy region. No pronounced dips or enhancements are observed. At a fixed energy the reaction cross section is expected to vary as $A^{2/3}$. Figure 4 displays our measured reaction cross sections divided by $A^{2/3}$; the errors associated with carbon, fluorine, aluminum, and silicon are not shown, but they have the same magnitude as those shown for the beryllium data. Except for beryllium, and perhaps fluorine, the measured cross sections indeed vary as $A^{2/3}$. The ⁹Be nucleus is essentially a pair of α particles and an extra neutron which is available for reactions. This probably accounts for the fact that the reaction cross section for ⁹Be is higher than that of ¹²C.

Figure 5 contains plots of $(\sigma_R/\pi)^{1/2}$ vs $A^{1/3}$ at four representative energies. Each plot has been fitted with the expression

$$\sigma_R = \pi (\gamma_0 A^{1/3} + \lambda)^2$$

where λ is the de Broglie wavelength of the incident proton. The average slope of all of the lines is given by $\gamma_0 = 1.21 \pm 0.03$ fm. In a similar study of the proton total reaction cross sections for medium-weight and heavy nuclei in the energy range 30 to 60 MeV, Menet *et al.*²⁴ found that the data could be fitted using the same expression but with $\gamma_0 = 1.23 \pm 0.01$ fm.

The optical model predictions of σ_R are in good agreement with the values measured for silicon and aluminum, the two heaviest nuclei studied in the experiment. Agreement is fair for carbon

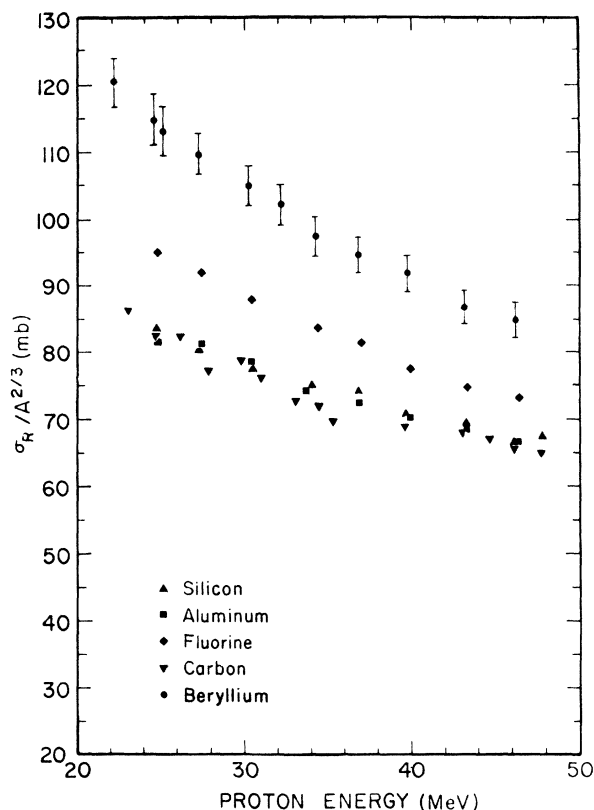


FIG. 4. Proton total reaction cross sections, measured in the present experiment, divided by $A^{2/3}$, plotted as a function of proton energy.

and for beryllium, the lightest nuclei studied. This decrease in the effectiveness of the model with decreasing A is not surprising, for the concept of an average potential produced by the nucleons in the nucleus becomes less realistic in the low A region.

There is some evidence²⁰ that in the case of $p + {}^{12}\text{C}$ resonances of the compound system ${}^{13}\text{N}$ influence the total reaction cross sections up to 30 MeV incident proton energy. It remains to be shown that such anomalous behavior in the

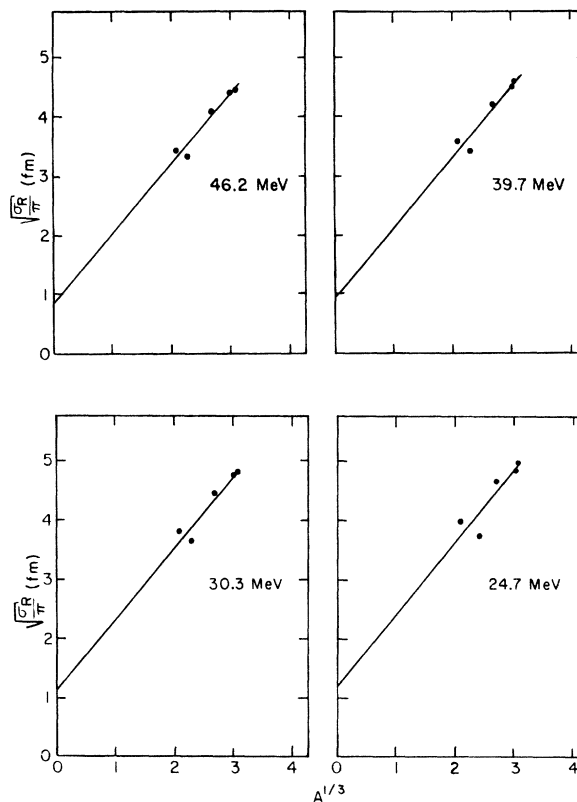


FIG. 5. $(\sigma_R/\pi)^{1/2}$ versus $A^{1/3}$, using results of the present experiment.

energy dependence of the reaction cross sections occurs also for other light nuclei. Because of the rather large energy steps chosen in the present experiment, no information could be obtained on this question.

The authors wish to express their gratitude to John Nimmo, Elsa Ginkel, Mike Wright, Fulton Wong, and Carl Ledbetter for their assistance in the accumulation and reduction of the data and in the calculations of the corrections.

*Work supported in part by the U. S. Atomic Energy Commission.

† Present address: Laboratoire de L'Accélérateur Linéaire, Faculté des Sciences, Orsay, France.

‡ Work supported in part by the Research Corporation and the Faculty Research Committee, University of Redlands, Redlands, California 92373.

§ Present address: U. S. Army Logistics Management Center, Fort Lee, Virginia 23801.

¶ Present address: University of Alberta, Edmonton 7, Alberta, Canada.

|| Permanent address: Institute "Ruder Bošković,"

Zagreb, Yugoslavia.

**Permanent address: Department of Physics, University of Manitoba, Winnipeg, Manitoba, Canada.

†† Present address: Veterans Administration Hospital, San Diego, California 92037.

***Work supported in part by the Research Corporation.

¹ For example, see P. E. Hodgson, *Ann. Rev. Nucl. Sci.* **17**, 1 (1967); F. G. Perey, *Phys. Rev.* **131**, 745 (1963).

² G. W. Greenlees, G. J. Pyle, and Y. C. Tang, *Phys. Rev. Lett.* **17**, 33 (1966); *Phys. Rev.* **171**, 1115 (1968); G. W. Greenlees, W. Makofske, and G. J. Pyle, *Phys. Rev. C* **1**, 1145 (1970).

- ³J. K. Dickens, D. A. Haner, and C. N. Waddell, *Phys. Rev.* **132**, 2159 (1963).
- ⁴R. M. Craig, J. C. Dore, G. W. Greenlees, J. Lowe, and D. L. Watson, *Nucl. Phys.* **79**, 177 (1966).
- ⁵T. Tamura and T. Terasawa, *Phys. Lett.* **8**, 41 (1964).
- ⁶J. Lowe and D. L. Watson, *Phys. Lett.* **23**, 261 (1966); **24B**, 174 (1967).
- ⁷B. Buck, *Phys. Rev.* **130**, 712 (1963).
- ⁸L. Rosen, J. G. Beery, A. S. Goldhaber, and E. H. Auerbach, *Ann. Phys. (N.Y.)* **34**, 96 (1965).
- ⁹M. P. Fricke, E. E. Gross, B. J. Morton, and A. Zucker, *Phys. Rev.* **156**, 1207 (1967).
- ¹⁰F. D. Becchetti, Jr., and G. W. Greenlees, *Phys. Rev.* **182**, 1190 (1969).
- ¹¹I. H. Sloan, *Nucl. Phys.* **A168**, 211 (1971).
- ¹²W. M. Kloet and J. A. Tjon, *Ann. Phys. (N.Y.)* (to be published).
- ¹³R. F. Carlson, W. F. McGill, T. H. Short, J. M. Cameron, J. R. Richardson, W. T. H. van Oers, J. W. Verba, P. Doherty, and D. J. Margaziotis, *Nucl. Inst.* (to be published).
- ¹⁴R. F. Carlson, P. Doherty, D. J. Margaziotis, I. Šlaus, S. Y. Tin, and W. T. H. van Oers, *Lett. Nuovo Cimento* **8**, 319 (1973).
- ¹⁵J. W. Verba, H. Willmes, R. F. Carlson, I. Šlaus, J. R. Richardson, and E. L. Petersen, *Phys. Rev.* **153**, 1127 (1967).
- ¹⁶H. Willmes, J. R. Richardson, I. Šlaus, and J. W. Verba, *Part. and Nuclei* **4**, 192 (1972).
- ¹⁷J. F. Dicello, G. J. Igo, and M. L. Roush, *Phys. Rev.* **157**, 1001 (1967).
- ¹⁸D. G. Montague, R. K. Cole, M. Makino, and C. N. Waddell, *Nucl. Phys.* **A199**, 457 (1973).
- ¹⁹R. E. Pollock and G. Schrank, *Phys. Rev.* **140**, B575 (1965).
- ²⁰M. Q. Makino, C. N. Waddell, and R. M. Eisberg, *Nucl. Phys.* **68**, 378 (1965).
- ²¹J. F. Dicello and G. Igo, *Phys. Rev. C* **2**, 488 (1970).
- ²²R. A. Giles and E. J. Burge, *Nucl. Phys.* **50**, 327 (1964).
- ²³M. Q. Makino, C. N. Waddell, and R. M. Eisberg, *Nucl. Phys.* **50**, 145 (1964).
- ²⁴J. J. H. Menet, E. E. Gross, J. J. Malanify, and A. Zucker, *Phys. Rev. C* **4**, 1114 (1971).
- ²⁵T. J. Gooding, *Nucl. Phys.* **12**, 241 (1959).
- ²⁶R. Chapman and A. M. Macleod, *Nucl. Phys.* **A94**, 313 (1967).
- ²⁷K. Bearpark, W. R. Graham, and G. Jones, *Nucl. Phys.* **73**, 206 (1965).
- ²⁸M. Q. Makino, C. N. Waddell, and R. M. Eisberg, *Bull. Am. Phys. Soc.* **12**, 1125 (1967).
- ²⁹I. E. Dayton and G. Schrank, *Phys. Rev.* **101**, 1358 (1956).
- ³⁰D. G. Montague, R. K. Cole, P. S. Lewis, and C. N. Waddell, *Nucl. Phys.* **A199**, 433 (1973).
- ³¹G. S. Mani, *Nucl. Phys.* **A165**, 145 (1971); **A165**, 384 (1971).
- ³²J. Benveniste, R. G. Finke, and E. A. Martinelli, *Phys. Rev.* **101**, 655 (1956).
- ³³R. W. Peelle, *Phys. Rev.* **105**, 1311 (1957).
- ³⁴W. W. Daehnick and R. Sherr, *Phys. Rev.* **133**, B934 (1964).
- ³⁵B. W. Ridley and J. F. Turner, *Nucl. Phys.* **58**, 497 (1958).
- ³⁶J. K. Dickens, D. A. Haner, and C. N. Waddell, *Phys. Rev.* **129**, 743 (1963).
- ³⁷L. N. Blumberg, E. E. Gross, A. van der Woude, A. Zucker, and R. H. Bassel, *Phys. Rev.* **147**, 812 (1966).
- ³⁸J. A. Fannon, E. J. Burge, D. A. Smith, and N. K. Ganguly, *Nucl. Phys.* **A97**, 263 (1967).
- ³⁹C. B. Fulmer, J. B. Ball, A. Scott, and M. L. Whiten, *Phys. Rev.* **181**, 1565 (1969).
- ⁴⁰T. Stovall and N. M. Hintz, *Phys. Rev.* **135**, B330 (1964).
- ⁴¹S. W. Chen and N. M. Hintz, in *The Proceedings of the International Conference on Nuclear Physics, Paris, 1958* (Dunod, Paris, 1958), p. 387.
- ⁴²E. L. Petersen, I. Šlaus, J. W. Verba, R. F. Carlson, and J. R. Richardson, *Nucl. Phys.* **A102**, 145 (1967).
- ⁴³R. Dittman, H. S. Sandhu, R. K. Cole, and C. N. Waddell, *Nucl. Phys.* **A126**, 592 (1969).
- ⁴⁴R. K. Cole, C. N. Waddell, R. R. Dittman, and H. S. Sandhu, *Nucl. Phys.* **75**, 241 (1966).
- ⁴⁵W. F. McGill and J. M. Cameron, private communication.
- ⁴⁶H. S. Sandhu, J. M. Cameron, and W. F. McGill, *Nucl. Phys.* **A169**, 600 (1971).
- ⁴⁷M. A. Melkanoff, J. S. Nodvik, D. S. Saxon, and R. D. Woods, *Phys. Rev.* **106**, 793 (1957).
- ⁴⁸G. R. Satchler, *Nucl. Phys.* **A100**, 497 (1967).
- ⁴⁹R. C. Barrett, A. D. Hill, and P. E. Hodgson, *Nucl. Phys.* **62**, 133 (1965).
- ⁵⁰A. E. Glassgold and P. J. Kellogg, *Phys. Rev.* **109**, 1291 (1958).
- ⁵¹H. W. Bertini, *Phys. Rev. C* **5**, 2118 (1972).
- ⁵²M. P. Fricke and G. R. Satchler, *Phys. Rev.* **139**, B567 (1965).